Study of Average Static Hold-up Along a Rotary Disc Contactor in the Presence of Nanoparticles

H. Molavi,[a,*] M. M. Moharrer,[b] M. R. Mozdianfard,[c] and H. Bahmanyar[d]

[a]Chemical and Material Center, Niroo Research Institute, Tehran, Iran
[b]Mechanical Engineering School, University of Tehran, Tehran, Iran
[c]Separation Processes Research Group, University of Kashan, Iran
[d]Faculty of Chemical Engineering, University of Tehran, Tehran, Iran

Original scientific paper
Received: July 7, 2013
Accepted: December 9, 2013

Regarding the important role of static hold-up in both hydrodynamic and mass transfer rate in extraction columns, average static hold-up has been studied in a Rotary Disc Contactor (RDC) as a function of rotor speed, average mother drop size and number of stages using several chemical systems. In the light of the promising potential of nanofluids in mass transfer applications, in a quite novel investigation, nanofluids were applied as dispersed phases to the RDC column. Two types of SiO_2 nanoparticles with different hydrophobicities were employed in nanofluids preparation, which stabilities were appraised by sedimentation method and UV-vis spectrophotometry. Transmission Electron Microscopy was also applied to examine the size and shape of SiO_2 nanoparticles.

Key words:
Static hold-up, stability of nanofluids, rotary disc contactor

Introduction

Rotary disc contactor (RDC) has been widely used for liquid-liquid extraction owing to its advantages such as high operational flexibility, efficiency, throughput, as well as low driving power and capital cost. As a key variable in liquid-liquid extraction columns, hold-up has been discussed in the literature in three categories: static, dynamic and total hold-up.[1] Static hold-up refers to that portion of the dispersed phase which is trapped under the discs,[2] while dynamic hold-up refers to the moving fraction of the dispersed phase. Total hold-up equals the sum of static and dynamic hold-ups.

There are a number of publications in which dynamic and total hold-ups of RDC have been studied.[1–11] However, so far, limited work has been carried out on static hold-up in this type of column; this is despite the fact that many researchers have claimed that this part of the total hold-up could have an important influence on drop coalescence, residence time, interfacial area and general efficiency of the column in mass transfer operations.[1,5,6,12,13]

In a previous work of the authors,[14] using three different chemical systems and a swarm of dispersed phase drops and in the condition of no mass transfer and no continuous phase flow, the average static hold-up in an RDC column was studied and two predictive correlations were proposed. The effects of physical properties, rotor speed, mother drop size, as well as number of stages in the column were considered in the correlations.

In case of immovable rotors, this was:

$$\bar{\phi}_{n'} = 2.4\times10^{-10}\cdot\left(\frac{\mu_d}{\mu_c}\right)\cdot\left(\frac{\Delta\rho}{\rho_c}\right)\cdot \left(\frac{\gamma\rho_d d_{32_0}}{\mu_d^2}\right)^{1.85}\cdot n'^{-0.45}+0.018 \quad (1)$$

And for the condition of rotating discs, it became:

$$\bar{\phi}_{n'} = 3.73\times10^{-11}\cdot\left(\frac{\mu_d}{\mu_c}\right)^{0.9}\cdot\left(\frac{\Delta\rho}{\rho_c}\right)^{2.2}\cdot \left(\frac{N\mu_c^3}{\rho_c\gamma^2}\right)^{-0.4}\cdot\left(\frac{\gamma\rho_d d_{32_0}}{\mu_d^2}\right)^{1.4}\cdot n'^{-0.2}+0.02 \quad (2)$$

According to the mentioned experimental work, the static hold-up proportion in the RDC was found to be comparable with total or dynamic hold-up of 20 %, considered as RDC normal operating condition by Ghalehchian and Slater.[4] Therefore, it was concluded that this part of total hold-up should not be neglected.[14]

Nanofluid, first introduced by Choi,[15] is a fluid in which nanometer-sized particles are suspended in a base fluid[16] and have some essential conditions,

*Telephone & Fax No.: +982188361604; Email: hmolavi@nri.ac.ir

such as homogeneous suspension, stability of suspension, low agglomeration of particles and no chemical change of the base fluid.[17]

Stability of nanofluids and quality of nanoparticles' dispersion in the base fluid are evaluated by various methods, namely conventional sedimentation method,[17,18] UV-vis spectrophotometry,[19–21] particle size analyzing,[17,22–24] and transmission electron microscopy (TEM).[22–24]

Several research studies on nanofluids have reported major changes in transport properties and improved heat transfer performances.[16,17,25–33] However, there are few investigations on mass transfer properties of nanofluids,[18,34–44] but indicate great potentials of their application. It is worth noting that such an investigation on the application of nanofluids to extraction columns is quite novel and the publications in this field are quite rare.[45–47]

In the present work, in order to study the application of nanofluids in mass transfer equipment, the average static hold-up in an RDC column was investigated using eight different nanofluids as dispersed phases. Furthermore, the effect of nanoparticles' presence on interfacial tension is discussed.

Experimental

Experimental setup

The glassy pilot RDC column with inner diameter and height of 91 mm and 100 cm, respectively, consisted of 21 rotors and 22 stators made from stainless steel. The outer and inner diameters of the rotors and stators were 4.55 cm and 6.1 cm, respectively, and the height of each compartment was 2.78 cm. Fig. 1 presents the schematic diagram of the experimental apparatus. More details on the experimental set-up have been presented in our pervious work.[14]

Materials

Two different base fluids (butyl acetate and toluene) and two types of SiO_2 nanoparticles (with different hydrophobicities) in two different volume fractions were used in the experiments; this led to ten distinct chemical systems (listed in Table 1).

The amorphous fumed hydrophobic and highly hydrophobic silica powders (HDK H20 and HDK H18, respectively) were of high purity with diameters in the range of 5–30 nm and density of 2200 kg m^{-3}. Their surfaces had been modified by $–OSi(CH_3)_2–$ groups. The shape and size of the H18 nanoparticles were examined by TEM.

In case of no mass transfer (no solute), distilled water and an organic phase were selected as the stagnant continuous phase and the dispersed phase,

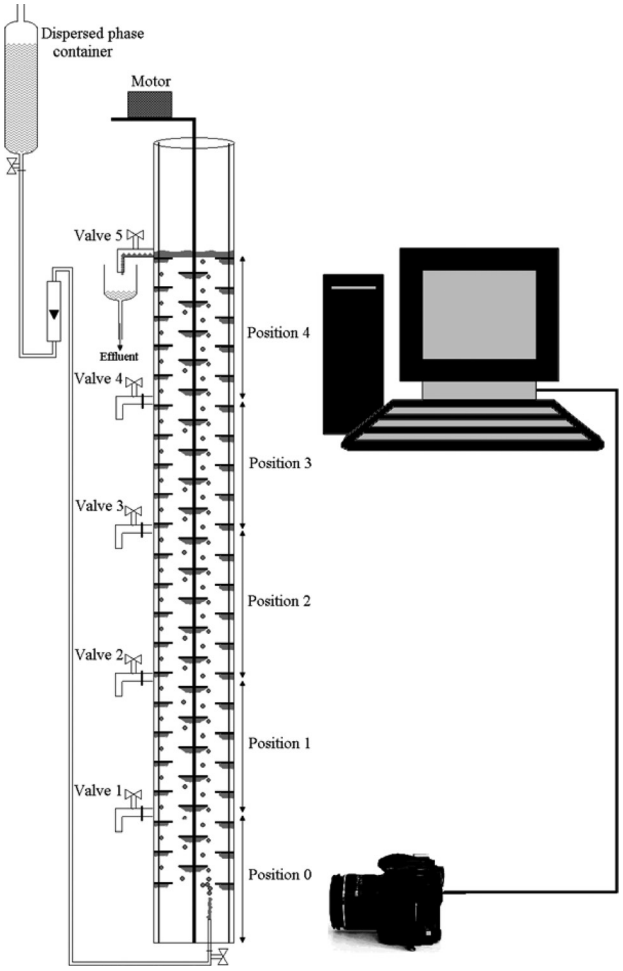

Fig. 1 – *Schematic diagram of the experimental set-up*

respectively. In order to ensure no mass transfer between organic and aqueous media, both phases were mutually saturated. SiO_2 nanoparticles were supplied from Wacker-Chemie to prepare the nanofluids. The different hydrophobicities and volume fractions of the nanoparticles allowed investigation of the effect of these parameters on average static hold-up.

At room temperature, densities of water, butyl acetate and toluene were 996, 875 and 860 kg m^{-3}, respectively, and similarly, their viscosities were found to be 0.87, 0.67 and 0.55 mPa s. The interfacial tensions of chemical systems without nanoparticles, i.e. W-B and W-T (see Table 1) were found to be 12.4 and 28 mN m^{-1}, respectively.

As it has been proven, viscosity and density of nanofluids with small values of nanoparticles in them are almost the same as those of pure base fluids.[28] Nanofluids' densities were measured in this study, but there was no significant change in the value (less than 0.3 %). Furthermore, their viscosities were calculated using the proposed equation by Heris *et al.*:[28]

$$\mu_{NF} = \mu_{BF} \cdot (1 + 2.5 \cdot 10^{-2} vol\,\%) \qquad (3)$$

Table 1 – *Chemical systems*

Chemical system name	Continuous phase	Dispersed phase
W-B	Water	Pure butyl acetate
W-BNF$_1$	Water	Butyl acetate + 0.05 vol % HDK-H18
W-BNF$_2$	Water	Butyl acetate + 0.2 vol % HDK-H18
W-BNF$_3$	Water	Butyl acetate + 0.05 vol % HDK-H20
W-BNF$_4$	Water	Butyl acetate + 0.2 vol % HDK-H20
W-T	Water	Pure toluene
W-TNF$_1$	Water	Toluene + 0.05 vol % HDK-H18
W-TNF$_2$	Water	Toluene + 0.2 vol % HDK-H18
W-TNF$_3$	Water	Toluene + 0.05 vol % HDK-H20
W-TNF$_4$	Water	Toluene + 0.2 vol % HDK-H20

Nanofluids preparation and stability

Ultrasonication as an external mechanical energy was used for dispersion of nanoparticles into the base fluid. For this, a Hielscher ultrasound generator (24 kHz, 400 W) was employed for 1hour by applying H14 sonotrode with 125 μm, 105 W cm^{-2} and 0.7 s pulse duration.

Evaluation of nanofluids stability was carried out by sedimentation method and using UV-vis spectrophotometry.

Experimental procedure

Local static hold-up was measured using the draining method explained in detail previously.[14] However, in order to have a glimpse at the experimental procedure, some explanations have been provided further herein (see also Fig. 1).

In each run of the experiments, the RDC was filled with continuous phase up to the last valve (namely 5th valve). By using a glassy nozzle at the bottom of the column, the dispersed phase was then fed as a swarm of drops to the RDC. Afterwards, the rotor discs speed was adjusted at a prescribed value (varied in the range of 0–373.5 rpm) by using a digital motor drive. After ensuring stable conditions, photographs were taken of the dispersed phase drops above the nozzle (called mother drops). The photographs were used to determine mother drops size using AutoCAD software.

Subsequently, measurement of the static hold-up for each position started by closing the valve of the nozzle and turning off the motor. In order to reach local static hold-up for a specific position, the whole liquid volume (consisting of aqueous phase and trapped organic phase) was then drained from the position's lower valve. Using a decanter, the organic and aqueous phases were separated, and the volume of each phase was determined. Finally, the static hold-up for each position was calculated using the following expression:

ϕ_{Lp} = Volume of dispersed phase in a specific position/(entire liquid volume in that specific position).

Also, the average static hold-up for the column with a specific number of stages in it was determined as the following expression:

$\overline{\phi}_{n'}$ = Total volume of dispersed phase in the column with a specific number of stages in it/(entire liquid volume in the column with a specific number of stages in it).

Results and discussion

TEM micrograph of H18 nanoparticles

Fig. 2 shows TEM micrograph for H18 nanoparticles, confirming that the particles were primarily spherical or nearly spherical, and their size was consistent with their nominal value.

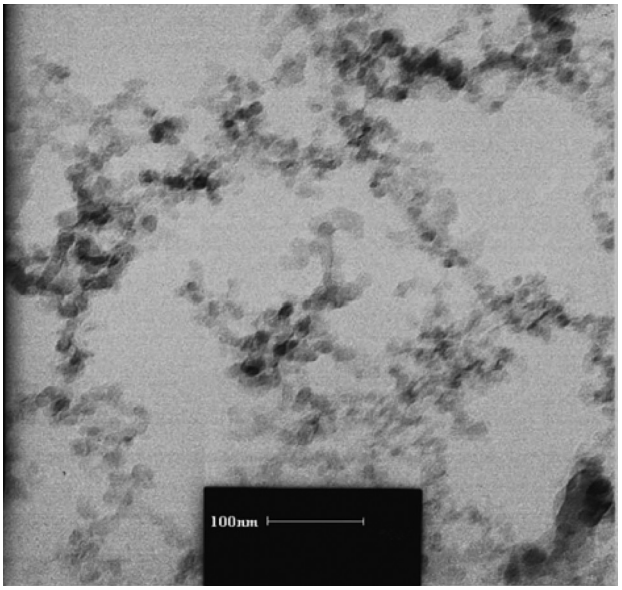

Fig. 2 – *TEM image of H18 nanoparticles*

Stability of nanofluids

The nanofluids' stability was evaluated using sedimentation method and UV-vis spectroscopy. The results of the sedimentation method are shown in Figs. 3 and 4, which proved that the nanofluids were stable for several days (at least 8 days). However, less stability was obtained for toluene-based nanofluids. It is worth noting that the nanofluids were applied to the column shortly after their preparation.

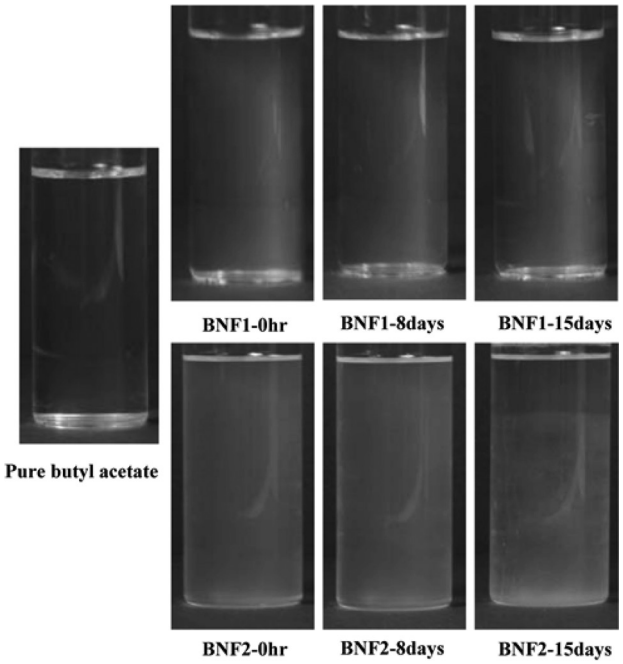

Fig. 3 – *Sedimentation method for appraising stability of butylacetate-based nanofluids*

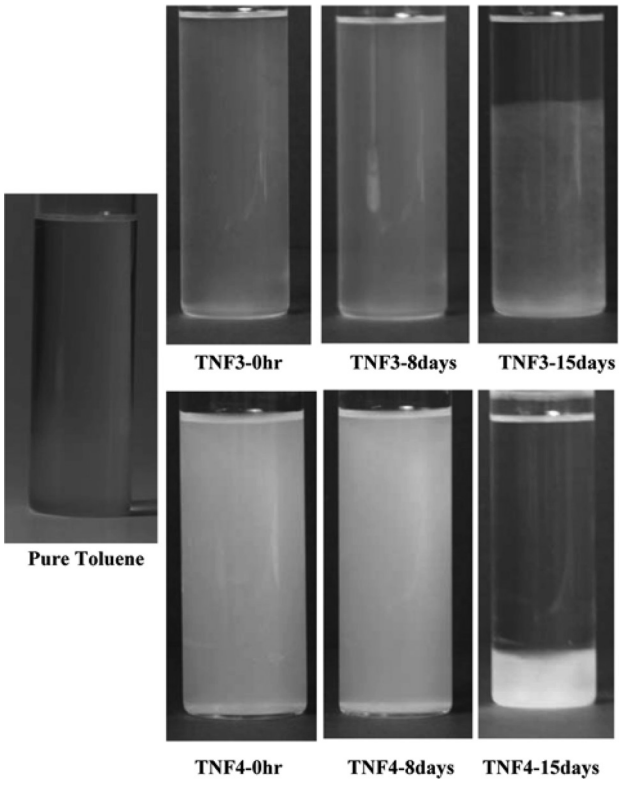

Fig. 4 – *Stability evaluation of toluene-based nanofluids using sedimentation method*

Furthermore, UV-vis spectroscopy results for evaluation of nanofluids stability for butyl acetate-based and toluene-based nanofluids are presented in Figs. 5 and 6, respectively, which confirm the stability of the nanofluids.

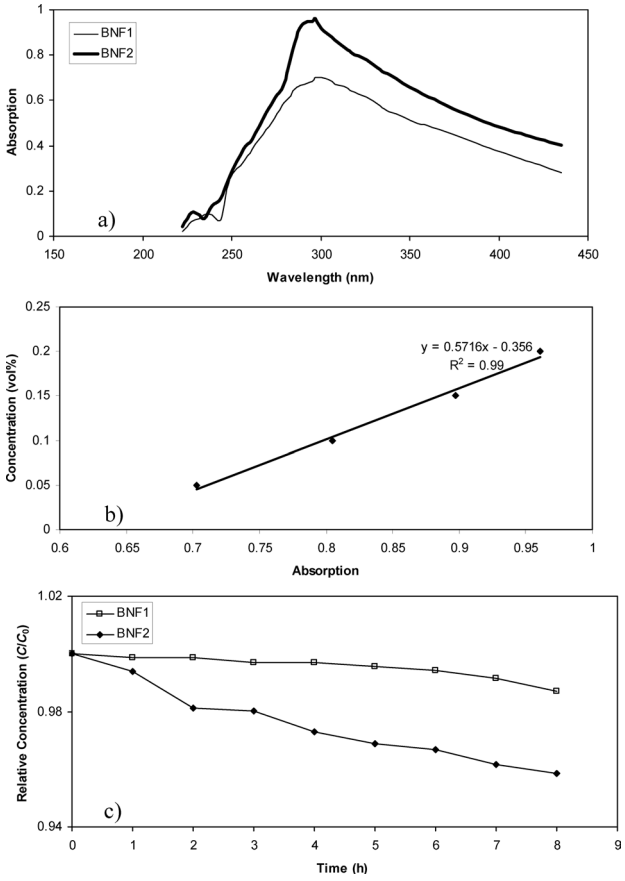

Fig. 5 – *a) UV-vis spectrum of butyl acetate-based nanofluids, b) Linear relationship between light absorption and concentration of H18 nanoparticles in butyl acetate suspension at wavelength of 296.8 nm, c) SiO_2 nanoparticles relative concentration versus time for butyl acetate-based nanofluids*

Regarding Figs. 5a and 6a, the absorbance peaks of butyl acetate and toluene nanofluids appear at 296.8 and 294.4 nm, respectively. The linear relationship between light absorbance and concentration of H18 nanoparticles in butyl acetate and H20 nanoparticles in toluene are presented in Figs. 5b and 6b, respectively. Figs. 5c and 6c demonstrate SiO_2 relative concentration versus time for butyl acetate-based and toluene-based nanofluids, respectively. Regarding Fig. 5c, the concentration of H18 nanoparticles in BNF_1 and BNF_2 samples reach 98.7 % and 95.8 % of the initial concentration after 8 hours, respectively. In addition, Fig. 6c shows that the relative concentrations of H20 nanoparticles in TNF_3 and TNF_4 reach 98.2 % and 95 % after 8 hours, respectively. Therefore, the samples are considered as stable nanofluids.

Interfacial tension and droplet geometry

As discussed previously,[45,46] adding SiO_2 nanoparticles to the organic phase leads to increase in interfacial tension of the water-organic chemical systems which results in more spherical drops. Similar behavior has been reported by Kim *et al*.[48] in bubble columns. Fig. 7 presents droplets sphericity

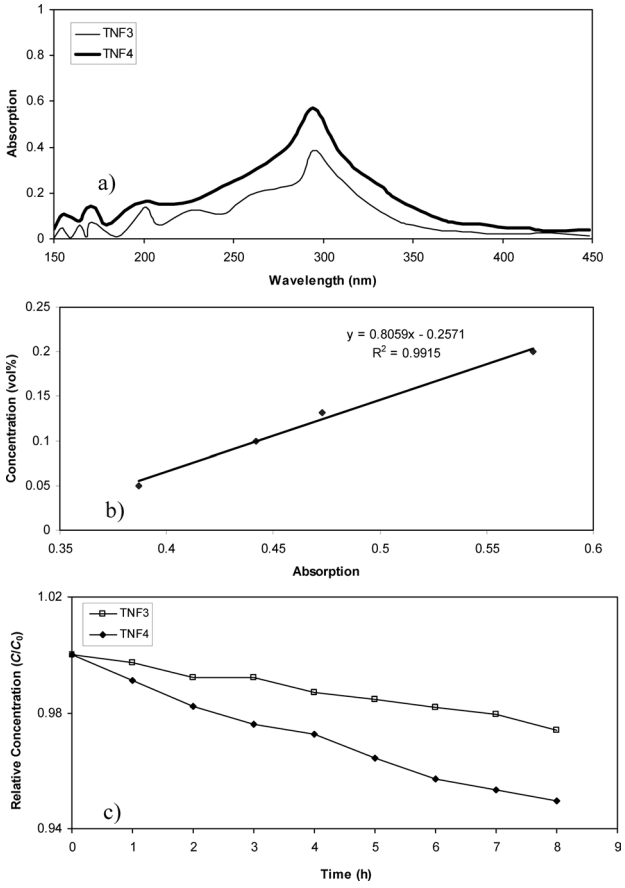

Fig. 6 – *a) UV-vis spectrum of toluene-based nanofluids, b) Linear relationship between light absorption and concentration of H20 nanoparticles in toluene-based nanofluids at wavelength of 294.4 nm, c) SiO_2 nanoparticles relative concentration versus time for toluene suspensions*

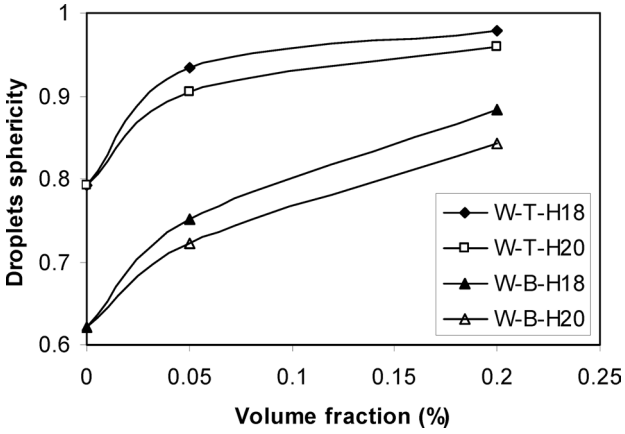

Fig. 7 – *Droplets sphericity versus nanoparticles volume fraction*

(defined as the ratio of the drop minor diameter to the drop major diameter) for W-T and W-B chemical systems, containing different concentrations of H18 and H20 nanoparticles. This parameter, which corresponds to interfacial tension, increases as the nanoparticle content increases. Also, more hydrophobic nanoparticles result in more droplet sphericity which indicates interfacial tension increase.

Average static hold-up

Fig. 8 demonstrates the static hold-up of the first and second stages of the RDC for two water-nanofluid chemical systems and at two different rotating speeds. As one can see, static hold-up (trapped organic phase under the discs and stators) decreases with an increase in rotor speed. Furthermore, the static hold-up amount is higher in the case of W-BNF_2, compared to that of W-BNF_4 chemical system. This is due to higher interfacial tension of the former chemical system, which is in accordance with Khoobi *et al.* results[46] for Water-Kerosene nanofluids chemical systems in a pulsed liquid-liquid extraction column.

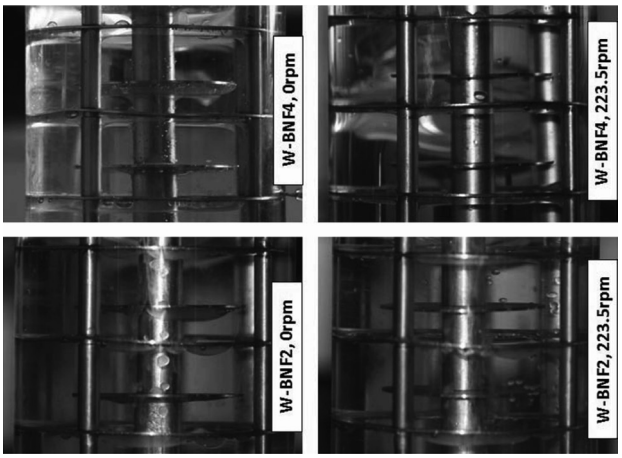

Fig. 8 – *Comparison of static hold-up for two water-nanofluid chemical systems at two different rotor speeds*

Average static hold-up amounts versus number of stages in the column for W-B and W-T, as well as associated nanofluid chemical systems, are presented in Figs. 9 and 10, respectively. The figures include chemical system, rotor speed, as well as mother drop size in their legends.

For all systems investigated, dependency of the average static hold-up on the number of stages in the column was found to be highest when rotors were turned off.

Figs. 11 and 12 compare the experimental average static hold-ups with calculated ones obtained from correlations (1) and (2). In the light of no access to interfacial tensions of water-nanofluid chemical systems, interfacial tensions of W-B and W-T chemical systems were used in hold-up calculations for water-butyl acetate and water-toluene nanofluids, respectively.

The absolute average relative error for correlations (1) and (2) were found to be 11.9 and 9.8 %, respectively. Furthermore, standard deviations for the mentioned correlations were 7.1 and 8 %, respectively. However, the deviations (using Eq. (4)) between calculated and experimental static hold-ups for W-T and water-toluene nanofluids (W-TNF_1 to W-TNF_4) were +3.11, +7.3, +24.6, +6.3 and +21.9,

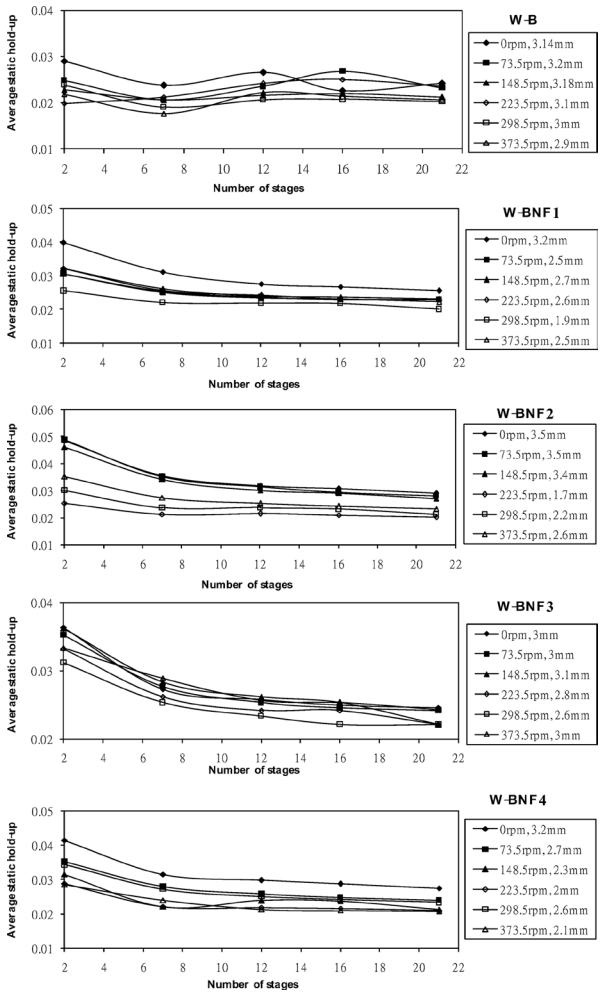

Fig. 9 – *Average static hold-up versus number of stages for W-B chemical systems*

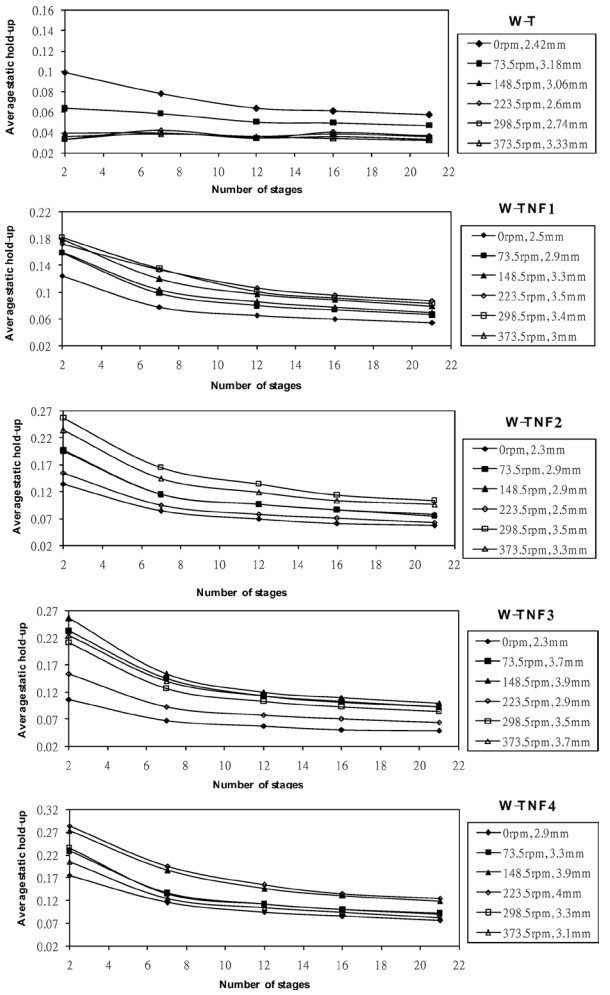

Fig. 10 – *Average static hold-up versus number of stages for W-T chemical systems*

respectively. The deviations for W-B and water-butyl acetate nanofluids (W-BNF$_1$ to W-BNF$_4$) were –1.39, +3.6, +10.4, +1.6 and +6.9, respectively.

$$Deviation = \frac{1}{n}\sum_{i=1}^{n}\left(\frac{y_{\exp}(i) - y_{calc}(i)}{y_{\exp}(i)}\right), \qquad (4)$$

Regarding Figs. 11 and 12 and also considering the deviation values, the increase in the volume fraction of the nanoparticles in the organic phase as well as the increase in the hydrophobicity of the nanoparticles, result in more deviation of experimental static hold-ups from calculated ones. This is in accordance with the increase in interfacial tension of the chemical systems discussed in section Interfacial tension and droplet geometry.

Afterwards, by substituting experimental hold-up and other parameters in eqs. (1) and (2), interfacial tensions of the water-nanofluids chemical systems were calculated. The results are presented in Table 2. As one can see, the maximum interfacial values are obtained for chemical systems with 0.2 % of H18 (highly hydrophobic) nanoparticles.

The increase in interfacial tension (IT) was determined using the following expression and the results are presented in the third column of Table 2, which show that adding SiO_2 hydrophobic and highly hydrophobic nanoparitcles to butyl acetate- and toluene-base fluids causes an increase of 2.5–21.3 % in water-nanofluids interfacial tension.

Table 2 – *Calculated interfacial tensions of the water-nanofluids chemical systems*

Chemical system	Interfacial tension (mN m^{-1})	Interfacial tension increment %
W-BNF$_1$	13.3	7.5
W-BNF$_2$	14.8	19.7
W-BNF$_3$	12.7	2.5
W-BNF$_4$	14.2	14.5
W-TNF$_1$	29.5	5.5
W-TNF$_2$	34	21.3
W-TNF$_3$	29.2	4.4
W-TNF$_4$	32.9	17.5

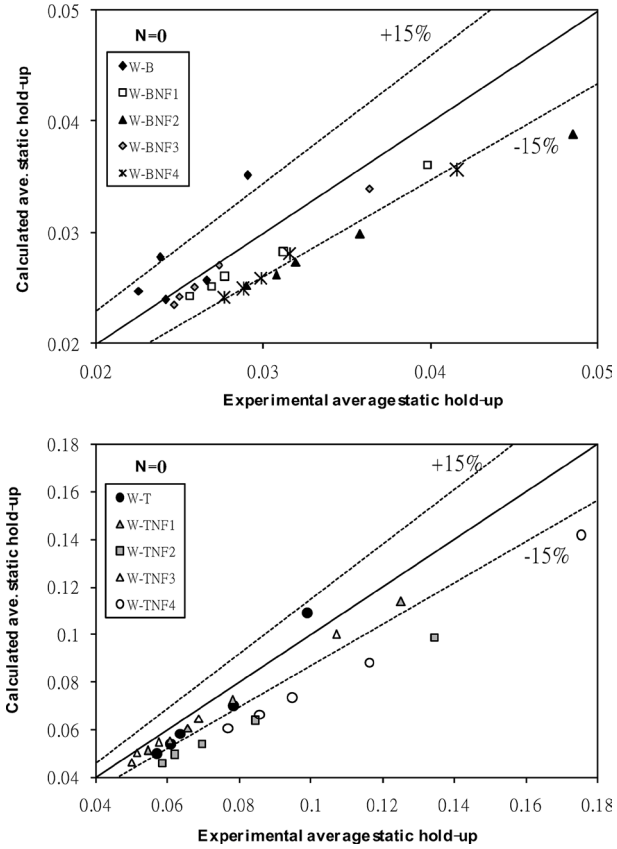

Fig. 11 – *Calculated average static hold-up by applying Eq. (1) versus experimental data in case of N = 0*

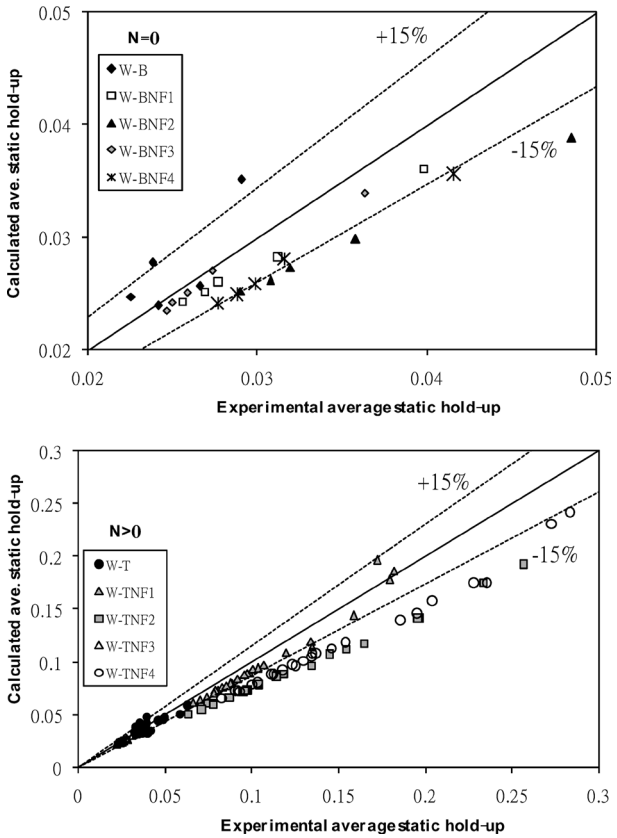

Fig. 12 – *Calculated average static hold-up by applying Eq. (2) versus experimental data in case of N>0*

Increase% = [calculated IT for nanofluid-aqueous phase − IT of aqueous phase-organic phase (without nanoparticles)] · 100%/IT of aqueous phase-organic phase.

Conclusion

Regarding nanofluids great potential for mass transfer applications, as well as the key role of static hold-up in both hydrodynamic and mass transfer rates in RDC columns, the average static hold-up was studied using eight Water-Nanofluids chemical systems, in an RDC as a quite novel work. The results were compared to the chemical systems containing no nanoparticles in their dispersed phase.

Nanofluids were prepared using a two-step procedure, and their stability was evaluated applying the sedimentation method and UV-vis spectrophotometry.

The results show that more hydrophobic nanoparticles lead to higher values of average static hold-up. Also, an increase in the amount of nanoparticles in the nanofluids has the same effect on this hydrodynamic parameter. It has been revealed that adding SiO_2 hydrophobic and highly hydrophobic nanoparitcles to butyl acetate- and toluene- base fluids would result in an increase of 2.5–21.3 % in water-nanofluids' interfacial tension.

Symbols used

d_{32_0} – Average mother drop size, m
n – Number of data, –
n' – Number of stages in the column, –
N – Rotor speed, rps
Vol % – Nanoparticles' volumetric content
y_{calc} – Calculated data
y_{exp} – Experimental data

Greek symbols

μ_{BF} – Viscosity of nanofluid base fluid, Pa s
μ_c – Viscosity of continuous phase, Pa s
μ_d – Viscosity of dispersed phase, Pa s
μ_{NF} – Viscosity of nanofluid, Pa s
ρ_c – Density of continuous phase, kg m^{-3}
ρ_d – Density of dispersed phase, kg m^{-3}
$\Delta\rho$ – Density difference, kg m^{-3}
$\overline{\phi}_{n'}$ – Average static hold-up for a column with n' stages, –
ϕ_{Lp} – Local static hold-up for a specific position, –
γ – Interfacial tension, N m^{-1}

References

1. *Puranik, S. S., Vogelpohl, A.,* Chem. Eng. Sci. **29** (1974) 501.
2. *Brodkorb, M. J., Slater, M. J.,* Trans. IChemE. **79A** (2001) 335.
3. *Attarakih, M. M., Bart, H. J., Lagar, L. G., Fagir, N. M.,* Chem. Eng. Process. **45** (2006) 113.
4. *Ghalehchian, J. S., Slater, M. J.,* Chem Eng. J. **75** (1999) 131.
5. *Jeffreys, G. V., Al-Aswad, K. K. M., Mumford, C. J.,* Separ. Sci. Technol. **16, 9** (1981) 1217.
6. *Kasatkin, A. G., Kagon, S. Z., Trukhanov, V. G.,* J. Appl. Chem. **6** (1962) 1903.
7. *Kulkarni, A. A., Gorasia, A. K., Ranade, V. V.,* Chem. Eng. Sci. **62** (2007) 7484.
8. *Laddha, G. S., Degaleesan, T. E., Kannappan, R.,* Can. J. Chem. Eng. **56, 4** (1978) 137.
9. *Moris, M. A., Diez, F. V., Coca, J.,* Sep. Purif. Technol. **11** (1997) 79.
10. *Murakami, A., Misonou, A., Inoue, K.,* Int. Chem. Eng. **18, 1** (1978) 16.
11. *Schmidt, S. A., Simon, M., Attarakih, M. M., Larger, L. G., Bart, H. J.,* Chem. Eng. Sci. **61** (2006) 246.
12. *Westerterp, K. R., Van Swaaij, W. P. M., Beenackers, A. A. C. M.,* Chemical Reactor Design and Operation, Wiley, New York, 1984.
13. *Yin, F., Afacan, A., Nandakumar, K., Chuang, K. T.,* Chem. Eng. Process. **41** (2002) 473.
14. *Molavi, H., Hoseinpour, S., Bahmanyar, H.,* Can. J. Chem. Eng. **89, 6** (2011) 1464.
15. *Choi, S. U. S., Singer, D. A., Wang, H. P.,* Am. Soc. Mech. Eng. **231** (1995) 99.
16. *Yu, W., France, D. M., Routbort, J. L., Choi, S. U. S.,* Heat Transfer Eng. **29** (2008) 432.
17. *Li, X., Zhu, D., Wang, X.,* J. Colloid Interface Sci. **310** (2007) 456.
18. *Lee, J. K., Koo, J., Hong, H., Kang, Y. T.,* Int. J. Refrig **33** (2010) 269.
19. *Hwang, Y., Park, H. S., Lee, J. K., Jung, W. H.,* Curr. Appl Phys. **6** (2006) 67.
20. *Hwang, Y., Lee, J. K., Lee, C. H., Jung, Y. M., Cheong, S. I., Lee, C. G., Ku, B. C., Jang, S. P.,* Thermochim. Acta **455** (2007) 70.
21. *Jiang, L., Gao, L., Sun, J.,* J. Colloid Interface Sci. **260** (2003) 89.
22. *Hwang, Y., Lee, J. K., Jeong, Y. M., Cheong, S. I., Ahn, Y. C., Kim, S. H.,* Powder Technol. **186** (2008) 145.
23. *Kim, H., Kim, J., Kim, M.,* Nucl. Eng. Technol. **38, 1** (2006) 61.
24. *Kim, C., Kwak, K.,* Korea-Aust. Rheol. J. **17, 2** (2005) 35.
25. *Choi, S. U. S., Zhang, Z. G., Yu, W., Lockwood, F. E., Grulke, E. A.,* Appl. Phys. Lett. **79** (2001) 2252.
26. *Das, S. K., Putra, N., Theisen, P., Roetzel, W.,* J. Heat Transfer **125** (2003) 567.
27. *Eastman, J. A., Choi, S. U. S., Li, S., Yu, W., Thompson, L. J.,* Appl. Phys. Lett. **78** (2001) 718.
28. *Heris, S. Z., Etemad, S. G., Esfahany, M. N.,* Int. Commun. Heat Mass Transfer **33** (2006) 529.
29. *Jang, S. P., Choi, S. U. S.,* Appl. Phys. Lett. **84** (2004) 4316.
30. *Kebelinski, P., Philipot, S. R., Choi, S. U. S., Eastman, J. A.,* Int. J. Heat Mass Transfer **45** (2002) 855.
31. *Wang, X., Xu, X., Choi, S. U. S.,* J. Thermophys. Heat Transfer **13** (1999) 474.
32. *Wen, D., Ding, Y.,* Int. J. Heat Mass Transfer **47** (2004) 5181.
33. *Xie, H., Lee, H., Youn, W., Choi, M.,* J. Appl. Phys. **94** (2003) 4967.
34. *Krishnamurthy, S., Bhattacharya, P., Phelan, P. E.,* Nano Lett. **6** (2006) 419.
35. *Saien, J., Bamdadi, H.,* Ind. Eng. Chem. Res. **51, 14** (2012) 5157.
36. *Wen, J., Jia, X., Feng, W.,* Chem. Eng. Technol. **28** (2005) 53.
37. *Olle, B., Bucak, S., Holmes, T. C., Bromberg, L., Hatton, A., Wang, D. I. C.,* Ind. Eng. Chem. Res. **45** (2006) 4355.
38. *Lee, J. K., Koo, J., Hong, H., Kang, Y. T.,* Int. J. Refig. **33** (2010) 269.
39. *Kang, Y. T., Kim, H. J., Lee, K. I.,* Int. J. Refig. **31** (2008) 850.
40. *Beiki, H., Esfahany, M. N., Etesami, N.,* Int. J. Therm. Sci. **64** (2013) 251.
41. *Kim, H., Jeong, J., Kang, Y. T.,* Int. J. Refig **35** (2012) 645.
42. *Saein, J., Bamdadi, H.,* Ind. Eng. Chem. Res. **51** (2012) 5157.
43. *Pang, C., Wu, W., Sheng, W., Zhang, H., Kang, Y. T.,* Int. J. Refig **35** (2012) 2240.
44. *Keshishian, N., Esfahany, M. N., Etesami, N.,* Int. Commun. Heat Mass Transfer **46** (2013) 148.
45. *Molavi, H., Bahmanyar, A., Khoobi, N., Bahmanyar, H.,* Can. J. Chem. Eng. **90, 3** (2012) 672.
46. *Khoobi, N., Bahmanyar, A., Molavi, H., Bastani, D., Mozdianfard, M. R., Bahmanyar, H.,* Can. J. Chem. Eng. **91, 3** (2013) 506.
47. *Bahmanyar, A., Khoobi, N., Mozdianfard, M. R., Bahmanyar, H.,* Chem. Eng. Process. **50** (2011) 1198.
48. *Kim, J. K., Jung, J. Y., Kang, Y. T.,* Int. J. Refrig **29** (2006b) 22.